Int. J. Open Problems Compt. Math., Vol. 19, No. 1, March 2026
Print ISSN: 1998-6262, Online ISSN: 2079-0376

A Stable and Convergent Implicit Finite Difference Scheme for Variable-Order Time-Fractional Convection–Diffusion Equations

Iqbal H. Jebril
Department of Mathematics, Al-Zaytoonah University of Jordan, Amman, 11733, Jordan
Email: i.jebril@zuj.edu.jo
Iqbal M. Batiha
Department of Mathematics, Al Zaytoonah University of Jordan,
Amman 11733, Jordan
Nonlinear Dynamics Research Center (NDRC), Ajman University,
Ajman 346, United Arab Emirates
E-mail: i.batiha@zuj.edu.jo

Received 12 June 2025; Accepted 08 December 2025

Abstract

This study develops and investigates an implicit finite difference approach (FDA) for solving a class of linear variable-order (VO) time-fractional partial differential equations (PDEs) that involve both convection and diffusion effects. The scheme is constructed by approximating the VO time-fractional derivative through a finite difference formulation and applying central difference operators for the spatial derivatives. A comprehensive theoretical analysis is carried out. By means of Fourier analysis, the method is shown to be unconditionally stable and convergent. In addition, the unique solvability of the resulting discrete system is demonstrated. To support the theoretical findings, several numerical experiments are presented, which confirm the accuracy, efficiency, and robustness of the proposed method.

Keywords: *Variable-order fractional derivative, Convection–diffusion equations, Stability analysis, Convergence analysis, Fourier analysis*

1 Introduction

Fractional calculus (FC), a branch of mathematical analysis that generalizes differentiation and integration to non-integer orders, dates back to a question posed by L'Hôpital to Leibniz in 1695 [1, 2]. For centuries, it remained mainly of theoretical interest to mathematicians such as Liouville, Riemann, and Grünwald [3, 4]. In recent decades, however, FC has become a vital tool for modeling complex systems in diverse scientific and engineering fields. Its ability to capture non-local interactions and memory effects provides an advantage over classical integer-order models in describing phenomena such as anomalous diffusion, viscoelasticity, signal processing, and fluid dynamics [5, 6, 7]. A notable extension of FC is VO-FO calculus, where the order of differentiation α is not constant but depends on time, space, or other variables, i.e., $\alpha(x, t)$ [8, 9]. This generalization offers a more flexible and accurate framework for modeling systems in which memory effects or physical processes vary dynamically [10, 11]. VO operators are, for example, effective in modeling diffusion in heterogeneous media with spatially varying rates or viscoelastic materials with temperature-dependent properties [12, 13]. The increasing interest in VO is reflected in extensive research on its theory and applications [14, 15].

Despite their modeling benefits, exact analytical solutions of VO-FO-PDEs are rarely obtainable, motivating the development of efficient numerical schemes [16, 17]. Among them, FDA are particularly popular due to their simplicity and effectiveness in discretizing operators [18, 19, 20, 21, 22]. The major challenge lies in discretizing the non-local FO derivative. Various schemes have been proposed, including Grünwald–Letnikov (GL)-based approximations [23, 24, 25, 26], and the widely used L_1 scheme for the Caputo derivative, noted for its simplicity and solid theoretical basis [27, 28]. Higher-order schemes such as L1-2 have also been introduced to improve accuracy [29]. For time-dependent problems, the choice between explicit and implicit schemes is crucial. Explicit schemes are simple but suffer from restrictive stability conditions, whereas implicit schemes generally provide better stability. Unconditionally stable schemes are particularly desirable since they impose no restriction on the time step relative to the spatial mesh size [30, 31]. Stability and convergence analysis of such schemes is essential, and Fourier/von Neumann analysis has been widely used for linear FO PDEs [32, 33]. To address the high computational cost from the non-local nature of FO operators, fast algorithms have also been developed [34, 35].

This work focuses on VO time-FO convection–diffusion equations (CDEs), which are important for modeling transport processes combining anomalous diffusion and convection with spatially and temporally varying characteristics [36, 37, 38]. While constant-order FO convection–diffusion equations have been extensively studied [39, 40], VO time FO-CDEs remain more challenging.

In addition, non-standard FDA schemes have been investigated to preserve key physical properties of the continuous models [41, 42]. Related problems, such as FO Burgers' equations, have also been widely explored, illustrating the broad applicability of these approaches [43, 44]. The paper is structured as follows: Section 2 introduces the mathematical preliminaries. Section 3 develops the implicit FDA and rigorously analyzes its stability, convergence, and solvability. Section 4 presents numerical results validating the theory. Section 5 concludes with final remarks.

2 Basic Concepts

This section provides the necessary mathematical definitions and concepts that form the foundation of the numerical scheme developed in this paper.

Definition 2.1 ([3, 17]) *For a sufficiently smooth function $v(t)$, the Caputo FO derivative of order $\alpha(x,t) > 0$ is defined as*

$$\frac{\partial^{\alpha(x,t)} v(x,t)}{\partial t^{\alpha(x,t)}} = \begin{cases} \dfrac{1}{\Gamma(m-\alpha(x,t))} \displaystyle\int_0^t (t-\xi)^{m-\alpha(x,t)-1} \frac{d^m v(x,\xi)}{d\xi^m}\, d\xi, & m-1 < \alpha(x,t) < m, \\ \dfrac{d^m v(x,t)}{dt^m}, & \alpha(x,t) = m \in \mathbb{N}, \end{cases} \tag{1}$$

where $\Gamma(\cdot)$ denotes the Gamma function and $m = \lceil \alpha(x,t) \rceil$ is the smallest integer greater than or equal to $\alpha(x,t)$.

Definition 2.2 ([8, 10]) *Let $\alpha(x,t)$ be a function defined such that $0 < \alpha(x,t) < 1$ for all x and t in the domain. The VO time-FO Caputo derivative of a function $v(x,t)$ is defined as :*

$$\frac{\partial^{\alpha(x,t)} v(x,t)}{\partial t^{\alpha(x,t)}} = \frac{1}{\Gamma(1-\alpha(x,t))} \int_0^t (t-\xi)^{-\alpha(x,t)} \frac{\partial v(x,\xi)}{\partial \xi} d\xi. \tag{2}$$

The non-local (integral) nature of the FO derivative necessitates a specialized discretization approach. A widely used first-order accurate approximation for the constant-order Caputo derivative is the L1 scheme.

Definition 2.3 ([27, 28]) *For a constant order $\alpha \in (0,1)$, the Caputo FO derivative at time $t = t_{j+1}$ can be approximated by the L_1 formula :*

$$\frac{\partial^{\alpha} v(x,t_{j+1})}{\partial t^{\alpha}} \approx \frac{k^{-\alpha}}{\Gamma(2-\alpha)} \sum_{n=0}^{j} b_n \left[v(x,t_{j+1-n}) - v(x,t_{j-n}) \right], \tag{3}$$

where the coefficients are given by $b_n = (n+1)^{1-\alpha} - n^{1-\alpha}$. The numerical scheme developed in this work is a generalization of this approach for a variable order $\alpha(x,t)$.

We now recall standard definitions related to the analysis of FDAs.

Definition 2.4 ([45]) *A FDA is said to be stable in a certain norm $\|\cdot\|$ if there exists a constant $C > 0$, independent of the spatial and temporal step sizes h and k, such that for any time level j:*

$$\|\mathbf{v}^j\| \leq C\|\mathbf{v}^0\|, \tag{4}$$

where $\mathbf{v}^j$ denotes the numerical solution vector at time t_j. If this condition holds for any choice of h and k, the scheme is called unconditionally stable.

Definition 2.5 ([46]) *A FDA is convergent if the numerical solution v_i^j approaches the exact solution $v(x_i, t_j)$ as the step sizes tend to zero. Formally, for any fixed point (x, t) in the domain:*

$$\lim_{h,k\to 0} \left| v(x_i, t_j) - v_i^j \right| = 0. \tag{5}$$

The scheme is said to converge with order p in space and order q in time if the global error is bounded by $\mathcal{O}(h^p + k^q)$.

Definition 2.6 ([45]) *The Fourier stability analysis is a technique used to assess the stability of linear FDAs, typically under the assumption of periodic boundary conditions. The method assumes the error can be expressed as a single Fourier mode, $E_i^j = \xi^j e^{\iota\theta x_i}$ (where $\iota^2 = -1$). The scheme is stable if the amplification factor ξ satisfies $|\xi| \leq 1$ for all real wave numbers θ .*

3 Problem Formulation

This section is devoted to the construction of an implicit FDA for solving a class of linear VO time-FO convection-diffusion equations. The discretization of the VO-FO derivative is based on the L_1 scheme concept [27, 28] (Definition 2.3), generalized for VO.

Consider the following initial-boundary value problem:

$$\begin{cases} \dfrac{\partial^{\alpha(x,t)} v}{\partial t^{\alpha(x,t)}} + a(x,t)\dfrac{\partial^2 v}{\partial x^2} + c(x,t)\dfrac{\partial v}{\partial x} = f(x,t), \quad 0 < x < L,\ t > 0, \\ v(0,t) = q(t), \quad v(L,t) = p(t), \\ v(x,0) = s(x), \end{cases} \tag{6}$$

where $\alpha(x,t) \in (0,1)$ is the variable FO order, and the operator $\frac{\partial^{\alpha(x,t)}}{\partial t^{\alpha(x,t)}}$ is the VO time-FO Caputo derivative as defined in Definition 2.2.

Let $\phi_1(h)$ and $\phi_2(k)$ be two strictly positive functions governing the spatial and temporal step sizes, respectively. We discretize the domain $[0, L] \times [0, T]$ by defining the grid points:

$$x_i = i\phi_1(h), \quad i = 0, 1, \ldots, M,$$
$$t_j = j\phi_2(k), \quad j = 0, 1, \ldots, N.$$

The discrete approximations of the functions are denoted as:

$$v(x_i, t_j) \approx v_i^j, \qquad f(x_i, t_j) \approx f_i^j,$$
$$a(x_i, t_j) \approx a_i^j, \qquad c(x_i, t_j) \approx c_i^j.$$

The core of the discretization lies in approximating the non-local VO time-FO Caputo derivative. Starting from its integral definition (2), we have:

$$\begin{aligned}\frac{\partial^{\alpha(x_i,t_{j+1})}v}{\partial t^{\alpha(x_i,t_{j+1})}} &= \frac{1}{\Gamma(1-\alpha(x_i,t_{j+1}))}\int_0^{t_{j+1}}(t_{j+1}-\xi)^{-\alpha(x_i,t_{j+1})}\frac{\partial v(x_i,\xi)}{\partial \xi}d\xi \\ &= \frac{1}{\Gamma(1-\alpha(x_i,t_{j+1}))}\sum_{s=0}^{j}\int_{t_s}^{t_{s+1}}(t_{j+1}-\xi)^{-\alpha(x_i,t_{j+1})}\frac{\partial v(x_i,\xi)}{\partial \xi}d\xi.\end{aligned}$$

On each subinterval $[t_s, t_{s+1}]$, we approximate the first-order time derivative using a backward finite difference:

$$\left.\frac{\partial v(x_i,\xi)}{\partial \xi}\right|_{\xi\in[t_s,t_{s+1}]} \approx \frac{v_i^{s+1}-v_i^s}{\phi_2(k)} + \mathcal{O}(\phi_2(k)). \tag{7}$$

Substituting (7) into the integral and evaluating the resulting Riemann–Liouville integral analytically yields the generalized L_1 formula:

$$\frac{\partial^{\alpha(x_i,t_{j+1})}v}{\partial t^{\alpha(x_i,t_{j+1})}} \approx \frac{\phi_2(k)^{-\alpha(x_i,t_{j+1})}}{\Gamma(2-\alpha(x_i,t_{j+1}))}\left[v_i^{j+1}-v_i^j+\sum_{n=1}^{j}(v_i^{j-n+1}-v_i^{j-n})\delta_i^{j+1}(n)\right], \tag{8}$$

where the coefficients are given by:

$$\delta_i^{j+1}(n) = (n+1)^{1-\alpha(x_i,t_{j+1})} - n^{1-\alpha(x_i,t_{j+1})}, \quad \text{for } n = 0, 1, \ldots, j. \tag{9}$$

These coefficients inherit the properties from the constant-order L_1 scheme (Definition 2.3), namely:

1. $\delta_i^{j+1}(0) = 1,$
2. $1 > \delta_i^{j+1}(1) > \delta_i^{j+1}(2) > \cdots > 0.$

For the spatial derivatives, we employ second-order central difference approximations:

$$\frac{\partial v(x_i,t_{j+1})}{\partial x} \approx \frac{v_{i+1}^{j+1}-v_{i-1}^{j+1}}{2\phi_1(h)} + \mathcal{O}(\phi_1(h)^2), \tag{10}$$

$$\frac{\partial^2 v(x_i,t_{j+1})}{\partial x^2} \approx \frac{v_{i+1}^{j+1}-2v_i^{j+1}+v_{i-1}^{j+1}}{\phi_1(h)^2} + \mathcal{O}(\phi_1(h)^2). \tag{11}$$

Substituting the approximations (8), (11), and (10) into the governing PDE (**??**) evaluated at (x_i, t_{j+1}) gives:

$$\frac{\phi_2(k)^{-\alpha(x_i,t_{j+1})}}{\Gamma(2-\alpha(x_i,t_{j+1}))}\left[v_i^{j+1}-v_i^j+\sum_{n=1}^{j}(v_i^{j-n+1}-v_i^{j-n})\delta_i^{j+1}(n)\right]$$
$$+\,a_i^j\left(\frac{v_{i+1}^{j+1}-2v_i^{j+1}+v_{i-1}^{j+1}}{\phi_1(h)^2}\right)+c_i^j\left(\frac{v_{i+1}^{j+1}-v_{i-1}^{j+1}}{2\phi_1(h)}\right)=f_i^{j+1}.$$

for $i = 1, \ldots, M-1$ and $j = 0, \ldots, N-1$.

To simplify the notation and analyze the scheme's properties (stability, convergence - see Definitions 2.4 & 2.5), we introduce the following dimensionless parameters:

$$r_i^{j+1} = a_i^j \cdot \frac{\phi_2(k)^{\alpha(x_i,t_{j+1})}\Gamma(2-\alpha(x_i,t_{j+1}))}{\phi_1(h)^2},$$

$$w_i^{j+1} = c_i^j \cdot \frac{\phi_2(k)^{\alpha(x_i,t_{j+1})}\Gamma(2-\alpha(x_i,t_{j+1}))}{2\phi_1(h)},$$

$$\rho_i^{j+1} = \phi_2(k)^{\alpha(x_i,t_{j+1})}\Gamma(2-\alpha(x_i,t_{j+1})).$$

Multiplying the entire equation by ρ_i^{j+1} and incorporating the initial and boundary conditions:

$$v_i^0 = s_i, \quad i = 0, \ldots, M,$$

$$v_0^{j+1} = q^{j+1}, \quad v_M^{j+1} = p^{j+1}, \quad j = 0, \ldots, N-1,$$

we obtain the final implicit finite difference scheme:

$$\begin{cases} (r_i^{j+1}-w_i^{j+1})v_{i-1}^{j+1} + (1-2r_i^{j+1})v_i^{j+1} + (r_i^{j+1}+w_i^{j+1})v_{i+1}^{j+1} = \\ \quad v_i^j - \sum_{n=1}^{j}(v_i^{j-n+1}-v_i^{j-n})\delta_i^{j+1}(n) + \rho_i^{j+1}f_i^{j+1}, \\ \quad\quad \text{for } i = 1, \ldots, M-1, \quad j = 0, \ldots, N-1, \\ v_0^{j+1} = q^{j+1}, \quad v_M^{j+1} = p^{j+1}, \\ v_i^0 = s_i. \end{cases} \tag{12}$$

This resulting system of linear algebraic equations is tridiagonal and will be shown to be uniquely solvable. Its stability and convergence will be analyzed in the next section using Fourier analysis (Definition 2.6).

4 Stability of the Approximate Scheme

In this section, we use the method of Fourier analysis to discuss the stability of the approximate scheme (12). Consider the following equation:

$$(r_i^{j+1}-w_i^{j+1})v_{i-1}^{j+1}+(1-2r_i^{j+1})v_i^{j+1}+(r_i^{j+1}+w_i^{j+1})v_{i+1}^{j+1} = v_i^j-\sum_{n=1}^{j}(v_i^{j-n+1}-v_i^{j-n})\delta_i^{j+1}(n)+\rho_i^{j+1}\mathscr{F}_i^{j+1}, \tag{13}$$

for $i = 1, \ldots, M-1$, $j = 1, \ldots, N-1$. We define the following function:

$$v^j(x) = \begin{cases} v_i^j & \text{if } x_{i-1/2} < x < x_{i+1/2},\ i = 1, \ldots, M-1; \\ 0 & \text{otherwise.} \end{cases}$$

$v^j(x)$ has the Fourier series expansion:

$$v^j(x) = \sum_{p=-\infty}^{+\infty} \xi^j(p)e^{2\pi ipx/L}, \quad j = 0, \ldots, N,$$

where

$$\xi^j(p) = \frac{1}{L}\int_0^L v^j(x)e^{-2\pi ipx/L}\,dx.$$

Assume that the solution of equation (12) has the form

$$v_i^j = \xi^j e^{i\theta hi}, \tag{14}$$

where $\theta = 2\pi p/L$, $i^2 = -1$. Substituting (14) into (13), we obtain

$$\xi^{j+1}\left(r_i^{j+1}(e^{i\theta h}+e^{-i\theta h}) + w_i^{j+1}(e^{i\theta h}-e^{-i\theta h}) + 1 - 2r_i^{j+1}\right) = \xi^j-\sum_{n=1}^{j}(\xi^{j-n+1}-\xi^{j-n})\delta_i^{j+1}(n). \tag{15}$$

This simplifies to

$$\xi^{j+1}\left(1-4r_i^{j+1}\sin^2\left(\frac{\theta h}{2}\right)+2iw_i^{j+1}\sin(\theta h)\right) = \xi^j-\sum_{n=1}^{j}(\xi^{j-n+1}-\xi^{j-n})\delta_i^{j+1}(n). \tag{16}$$

Equation (16) can be rewritten as

$$\xi^{j+1} = \frac{\xi^j-\sum_{n=1}^{j}(\xi^{j-n+1}-\xi^{j-n})\delta_i^{j+1}(n)}{1-4r_i^{j+1}\sin^2\left(\frac{\theta h}{2}\right)+2iw_i^{j+1}\sin(\theta h)}. \tag{17}$$

Theorem 4.1 *The implicit FDA* (12) *is unconditionally stable for* $0 < \alpha(x,t) < 1$ *if there exists* $C > 0$ *such that* $\|v^j\|_2 = |\xi^j| \leq C\|v^0\|_2 = C|\xi^0|$, *for* $j = 1, 2, \ldots, N$.

Proof 4.2 *We prove by induction. For* $j = 1$, *from* (17),

$$\begin{aligned} |\xi^1| &= \left| \frac{\xi^0}{1 - 4r_i^1 \sin^2\left(\frac{\theta h}{2}\right) + 2iw_i^1 \sin(\theta h)} \right| \\ &= \frac{|\xi^0|}{\sqrt{16\left[(r_i^1)^2 - (w_i^1)^2\right] \sin^4\left(\frac{\theta h}{2}\right) + 8\left[2(w_i^1)^2 - r_i^1\right] \sin^2\left(\frac{\theta h}{2}\right) + 1}} \\ &= C_i^0 |\xi^0| \leq C|\xi^0|. \end{aligned} \tag{18}$$

where $C = \max_{0 \leq i \leq M} C_i^0$. *Assume the statement holds for* $j = 1, 2, \ldots, N$:

$$|\xi^j| \leq C|\xi^0|. \tag{19}$$

Now prove for $j + 1$:

$$|\xi^{j+1}| = \left| \frac{\xi^j - \sum_{n=1}^{j}(\xi^{j-n+1} - \xi^{j-n})\delta_i^{j+1}(n)}{1 - 4r_i^{j+1} \sin^2\left(\frac{\theta h}{2}\right) + 2iw_i^{j+1} \sin(\theta h)} \right| \tag{20}$$

$$= \frac{\left|\xi^j - \sum_{n=1}^{j}(\xi^{j-n+1} - \xi^{j-n})\delta_i^{j+1}(n)\right|}{\sqrt{16\left[(r_i^{j+1})^2 - (w_i^{j+1})^2\right] \sin^4\left(\frac{\theta h}{2}\right) + 8\left[2(w_i^{j+1})^2 - r_i^{j+1}\right] \sin^2\left(\frac{\theta h}{2}\right) + 1}}. \tag{21}$$

This is

$$\begin{aligned} |\xi^{j+1}| &= C_i^j \left| \xi^j - \sum_{n=1}^{j} (\xi^{j-n+1} - \xi^{j-n})\delta_i^{j+1}(n) \right| \\ &\leq C^j|\xi^j| + \sum_{n=1}^{j} \left(|\xi^{j-n+1}| + |\xi^{j-n}|\right) |\delta_i^{j+1}(n)| \\ &\leq C^j (2j+1) \, |\xi^0| \\ &\leq C \, |\xi^0|. \end{aligned} \tag{22}$$

where

$$C_i^j = \frac{1}{\sqrt{16\left[(r_i^{j+1})^2 - (w_i^{j+1})^2\right] \sin^4\left(\frac{\theta h}{2}\right) + 8\left[2(w_i^{j+1})^2 - r_i^{j+1}\right] \sin^2\left(\frac{\theta h}{2}\right) + 1}}. \tag{23}$$

$C^j = \max_{0\le i\le M} C_i^j$, *and* $C = \max_{0\le j\le N-1}(2j+1)C^j, i = 0,\dots,M,\ j = 0,\dots,N-1$. *Thus,* $|\xi^{j+1}| \le C|\xi^0|$ *for* $j = 0,\dots,N-1$, *and the scheme* (12) *is unconditionally stable.*

We use the method of Fourier analysis to discuss the convergence of the approximate scheme. Define the error as

$$e_i^j = v(x_i,t_j) - v_i^j. \tag{24}$$

Substituting into (13), we obtain

$$(r_i^{j+1}-w_i^{j+1})e_{i-1}^{j+1}+(1-2r_i^{j+1})e_i^{j+1}+(r_i^{j+1}+w_i^{j+1})e_{i+1}^{j+1} = e_i^j-\sum_{n=1}^{j}(e_i^{j-n+1}-e_i^{j-n})\delta_i^{j+1}(n)+\epsilon_i^j, \tag{25}$$

for $i = 1,\dots,M-1$, $j = 1,\dots,N-1$, where

$$\epsilon_i^j = \phi_2(k)^{\alpha(x_i,t_{j+1})}\Gamma(2-\alpha(x_i,t_{j+1}))[\mathcal{O}(\phi_2(k))+\mathcal{O}(\phi_1(h))].$$

We define the grid functions:

$$e^j(x) = \begin{cases} e_i^j & \text{if } x_{i-1/2} < x < x_{i+1/2},\ i = 1,\dots,M-1; \\ 0 & \text{otherwise,} \end{cases}$$

and

$$\epsilon^j(x) = \begin{cases} \epsilon_i^j & \text{if } x_{i-1/2} < x < x_{i+1/2},\ i = 1,\dots,M-1; \\ 0 & \text{otherwise.} \end{cases}$$

Then, $e^j(x)$ and $\epsilon^j(x)$ have Fourier series expansions:

$$e^j(x) = \sum_{p=-\infty}^{+\infty}\gamma^j(p)e^{2\pi ipx/L}, \quad \epsilon^j(x) = \sum_{p=-\infty}^{+\infty}\lambda^j(p)e^{2\pi ipx/L}, \quad j = 0,\dots,N, \tag{26}$$

where

$$\gamma^j(p) = \frac{1}{L}\int_0^L e^j(x)e^{-2\pi ipx/L}\,dx, \quad \lambda^j(p) = \frac{1}{L}\int_0^L \epsilon^j(x)e^{-2\pi ipx/L}\,dx. \tag{27}$$

We have

$$\int_0^L |e^j(x)|^2\,dx = \sum_{p=-\infty}^{+\infty}|\gamma^j(p)|^2, \quad \int_0^L |\epsilon^j(x)|^2\,dx = \sum_{p=-\infty}^{+\infty}|\lambda^j(p)|^2, \quad j = 0,\dots,N,$$

$$\|e^j\|_2^2 = \sum_{i=1}^{M-1}|\phi_1(h)e_i^j|^2 = \sum_{p=-\infty}^{+\infty}|\gamma^j(p)|^2, \quad j = 0,\dots,N, \tag{28}$$

$$\|\epsilon^j\|_2^2 = \sum_{i=1}^{M-1} |\phi_1(h)\epsilon_i^j|^2 = \sum_{p=-\infty}^{+\infty} |\lambda^j(p)|^2, \quad j = 0, \ldots, N. \tag{29}$$

Assume

$$e_i^j = \gamma^j e^{i\theta h i}, \quad \epsilon_i^j = \lambda^j e^{i\theta h i}. \tag{30}$$

Substituting into (22), we obtain

$$\gamma^{j+1}\left(r_i^{j+1}(e^{i\theta h} + e^{-i\theta h}) + w_i^{j+1}(e^{i\theta h} - e^{-i\theta h}) + 1 - 2r_i^{j+1}\right) = \gamma^j - \sum_{n=1}^{j}(\gamma^{j-n+1} - \gamma^{j-n})\delta_i^{j+1}(n) + \lambda^j. \tag{31}$$

Equation (27) can be rewritten as

$$\gamma^{j+1} = \frac{\gamma^j - \sum_{n=1}^{j}(\gamma^{j-n+1} - \gamma^{j-n})\delta_i^{j+1}(n) + \lambda^j}{1 - 4r_i^{j+1}\sin^2\left(\frac{\theta h}{2}\right) + 2iw_i^{j+1}\sin(\theta h)}. \tag{32}$$

Theorem 4.3 *The implicit FDA (12) is convergent for $0 < \alpha(x,t) < 1$ if $\|e^j\|_2 = |\gamma^j| \le C^*(\phi_1(h) + \phi_2(k))$, for $j = 1, 2, \ldots, N$, where $\phi_1(h) + \phi_2(k) \to 0$ as $(h,k) \to (0,0)$.*

Proof 4.4 *We prove by induction. For $j = 1$,*

$$\begin{aligned} |\gamma^1| &= \left| \frac{\gamma^0 + \lambda^0}{1 - 4r_i^1 \sin^2\left(\frac{\theta h}{2}\right) + 2iw_i^1 \sin(\theta h)} \right| \\ &= \frac{|\gamma^0 + \lambda^0|}{\sqrt{16\left[(r_i^1)^2 - (w_i^1)^2\right]\sin^4\left(\frac{\theta h}{2}\right) + 8\left[2(w_i^1)^2 - r_i^1\right]\sin^2\left(\frac{\theta h}{2}\right) + 1}} \\ &\le \frac{|\lambda^0|}{\sqrt{16\left[(r_i^1)^2 - (w_i^1)^2\right]\sin^4\left(\frac{\theta h}{2}\right) + 8\left[2(w_i^1)^2 - r_i^1\right]\sin^2\left(\frac{\theta h}{2}\right) + 1}}. \end{aligned} \tag{33}$$

since $\gamma^0 = e_i^0 = v(x_i, 0) - v_i^0 = 0$.

From the local truncation error, there exists $T > 0$ such that $|\epsilon_i^0| \le T(\phi_1(h) + \phi_2(k))$, for $i = 0, \ldots, M$. Thus,

$$\|\epsilon^0\|_2 = |\lambda^0| \le T\sqrt{L}(\phi_1(h) + \phi_2(k)),$$

and

$$|\gamma^1| \le \frac{T\sqrt{L}(\phi_1(h) + \phi_2(k))}{\sqrt{16[(r_i^1)^2 - (w_i^1)^2]\sin^4\left(\frac{\theta h}{2}\right) + 8[2(w_i^1)^2 - r_i^1]\sin^2\left(\frac{\theta h}{2}\right) + 1}} \le C^*(\phi_1(h) + \phi_2(k)),$$

where

$$C^* = \max_{0\le i\le M} \frac{T\sqrt{L}}{\sqrt{16[(r_i^1)^2-(w_i^1)^2]\sin^4\left(\frac{\theta h}{2}\right)+8[2(w_i^1)^2-r_i^1]\sin^2\left(\frac{\theta h}{2}\right)+1}}.$$

Assume it holds for $j = 1, \ldots, N$*:*

$$|\gamma^j| \le C^*(\phi_1(h)+\phi_2(k)). \tag{34}$$

Now prove for $j+1$*:*

$$\begin{aligned}|\gamma^{j+1}| &= \frac{\left|\gamma^j - \sum_{n=1}^{j}\left(\gamma^{j-n+1}-\gamma^{j-n}\right)\delta_i^{j+1}(n)+\lambda^j\right|}{\sqrt{16\big[(r_i^{j+1})^2-(w_i^{j+1})^2\big]\sin^4\big(\frac{\theta h}{2}\big)+8\big[2(w_i^{j+1})^2-r_i^{j+1}\big]\sin^2\big(\frac{\theta h}{2}\big)+1}}\\ &\le C_i^{j+1}\Big(|\gamma^j| + \sum_{n=1}^{j}\left(|\gamma^{j-n+1}|+|\gamma^{j-n}|\right)|\delta_i^{j+1}(n)|+|\lambda^j|\Big),\end{aligned} \tag{35}$$

Using the induction hypothesis and $|\epsilon_i^j| \le T(\phi_1(h)+\phi_2(k))$, $\|\epsilon^j\|_2 = |\lambda^j| \le T\sqrt{L}(\phi_1(h)+\phi_2(k))$*, we get*

$$\begin{aligned}|\gamma^{j+1}| &\le C_i^j\big[C^*(2j+1)+T\sqrt{L}\big]\big(\phi_1(h)+\phi_2(k)\big)\\ &\le C^j\big[C^*(2j+1)+T\sqrt{L}\big]\big(\phi_1(h)+\phi_2(k)\big)\\ &\le C^*\big(\phi_1(h)+\phi_2(k)\big).\end{aligned} \tag{36}$$

after adjusting C^* *appropriately, where* C_i^j, C^j *are defined as before. Thus, the scheme* (12) *is convergent.*

Theorem 4.5 *The approximate scheme* (12) *is uniquely solvable.*

Proof 4.6 *Suppose, for the sake of contradiction, that the tridiagonal matrix* A *corresponding to the linear system in* (12) *at a given time step is singular.*

$$A = \begin{pmatrix} 1-2r_1^{j+1} & r_1^{j+1}+w_1^{j+1} & 0 & \cdots & 0\\ r_2^{j+1}-w_2^{j+1} & 1-2r_2^{j+1} & r_2^{j+1}+w_2^{j+1} & \ddots & \vdots\\ 0 & r_3^{j+1}-w_3^{j+1} & 1-2r_3^{j+1} & \ddots & 0\\ \vdots & \ddots & \ddots & \ddots & r_{M-1}^{j+1}+w_{M-1}^{j+1}\\ 0 & \cdots & 0 & r_{M-1}^{j+1}-w_{M-1}^{j+1} & 1-2r_{M-1}^{j+1}\end{pmatrix} \tag{37}$$

Then, there exists a non-trivial vector $v = (v_1, v_2, \dots, u_{M-1})^T$ *such that* $Av = 0$*, with* $u_0 = u_M = 0$*.*

Assuming constant coefficients for simplicity (the variable case follows similarly via perturbation arguments), we employ the discrete sine transform, suitable for Dirichlet boundary conditions. The eigenmodes are given by $v_i^{(\mathfrak{m})} = \sin(\pi \mathfrak{m} i/M)$ *for* $\mathfrak{m} = 1, 2, \dots, M-1$*. The corresponding symbol (Fourier multiplier) is*

$$1 - 4r_i^{j+1} \sin^2\left(\frac{\pi\mathfrak{m}}{2M}\right) + 2iw_i^{j+1} \sin\left(\frac{\pi\mathfrak{m}}{M}\right). \tag{38}$$

For the matrix to be singular, this symbol must vanish for some $\mathfrak{m} \in \{1, 2, \dots, M-1\}$*. Setting the real and imaginary parts to zero yields:*

$$1 - 4r_i^{j+1} \sin^2\left(\frac{\pi\mathfrak{m}}{2M}\right) = 0, \quad 2w_i^{j+1} \sin\left(\frac{\pi\mathfrak{m}}{M}\right) = 0. \tag{39}$$

From the imaginary part, either $w_i^{j+1} = 0$ *or* $\sin(\pi\mathfrak{m}/M) = 0$*. The latter implies* $\pi\mathfrak{m}/M = k\pi$ *for integer* k*, so* $\mathfrak{m} = kM$*, which contradicts* $\mathfrak{m} < M$*.*

If $w_i^{j+1} = 0$*, the real part becomes* $1 - 4r_i^{j+1}\sin^2(\pi\mathfrak{m}/(2M)) = 0$*, so* $\sin^2(\pi\mathfrak{m}/(2M)) = 1/(4r_i^{j+1})$*. This requires* $r_i^{j+1} \geq 1/4$*, and the specific match with the discrete sine values, but as before, the condition* $\sin^2(\beta) = 1/(4r_i^{j+1})$ *combined with the imaginary constraint leads to the same contradiction since it reduces to cases where* $\mathfrak{m}/M$ *would need to be an odd integer divided by 2, impossible for* $\mathfrak{m} < M$*.*

Since no such $\mathfrak{m}$ *exists that makes the symbol zero,* A *has no zero eigenvalues and is thus nonsingular. Therefore, the system admits a unique solution at each time step.*

5 Application Results

This section presents a series of numerical experiments designed to validate the accuracy, convergence, and practical utility of the proposed implicit FDA (12). We consider several VO time-fractional PDEs and evaluate the performance of the method by comparing numerical solutions against exact solutions. The maximum absolute error (L_∞ norm) at the final time $t = T$ is used to quantify accuracy:

$$E_\infty(T) = \max_{0 \leq i \leq M} \left| u(x_i, T) - u_i^N \right|, \tag{40}$$

where $u(x_i, T)$ is the exact solution and u_i^N is the numerical approximation at the grid point (x_i, T). The numerical convergence rate is computed as:

$$\text{Rate} = \log_2\left(\frac{E(M,N)}{E(2M,2N)}\right), \tag{41}$$

with $E(M,N)$ denoting the maximum error for M spatial and N temporal steps. All simulations were implemented in Python using the NumPy and SciPy libraries within a Jupyter environment.

Example 5.1 *Consider the linear inhomogeneous time-fractional equation* (6) *on the domain* $(x,t) \in [0,1] \times [0,1]$, *with variable order* $\alpha(x,t) = \frac{2+\cos(x+t)}{4}$ *and exact solution:*

$$u(x,t) = x^2 + 2\frac{\Gamma(\alpha(x,t)+1)}{\Gamma(2\alpha(x,t)+1)}t^{\alpha(x,t)}.$$

Numerical solutions were computed at $T = 1$ *for various grid sizes with* $M = N$. *Table 1 reports the maximum absolute errors and convergence rates. The results confirm that the error decreases under grid refinement, and the scheme achieves a first-order convergence rate, consistent with the theoretical expectations for the* L_1*-type approximation.*

Figure 1 compares the numerical and exact solutions at $T = 1$ *for* $M = N = 40$, *showing excellent agreement. Figure 2 displays the surface plot of the absolute error, which remains small throughout the domain.*

Table 1: Maximum absolute errors and convergence rates for Example 1 at $T = 1$.

$M = N$	$\phi_1(h)$	E_∞	Rate
10	1.00E-01	8.52E-03	–
20	5.00E-02	4.31E-03	0.98
40	2.50E-02	2.17E-03	0.99
80	1.25E-02	1.09E-03	1.00
160	6.25E-03	5.46E-04	1.00

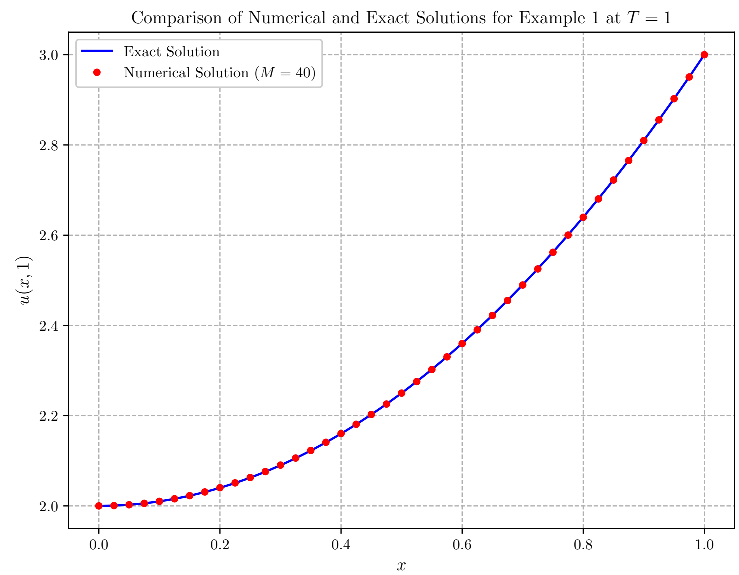

Figure 1: Comparison of numerical and exact solutions for Example 1 at $T = 1$ with $M = N = 40$.

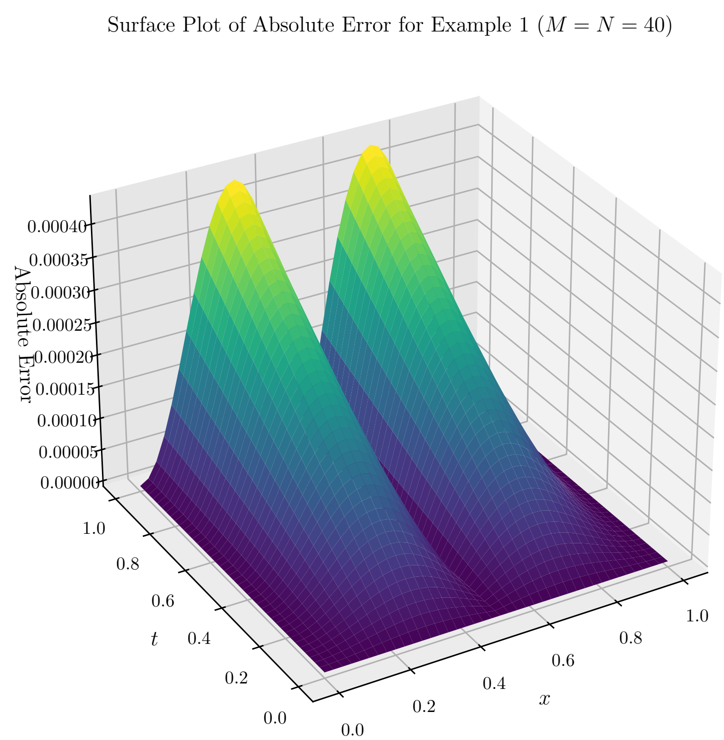

Figure 2: Surface plot of the absolute error for Example 1 at $T = 1$ with $M = N = 40$.

Example 5.2 *We now apply the scheme to the one-dimensional linear inhomogeneous FO Burgers' equation* (6) *on* $(x,t) \in [0,1] \times [0,1]$, *with VO* $\alpha(x,t) = \frac{\sin^2(xt)}{4}$ *and exact solution* $u(x,t) = x^2 + t^2$. *Table 2 presents the maximum absolute errors and convergence rates at* $T = 1$. *The scheme again exhibits stable behavior and first-order convergence.*

Figure 3 shows surface plots of the numerical and exact solutions at $T = 1$ *for* $M = N = 50$. *The surfaces are nearly indistinguishable, confirming the high accuracy of the method.*

Table 2: Maximum absolute errors and convergence rates for Example 2 at $T = 1$.

$M = N$	$\phi_1(h)$	E_∞	Rate
10	1.00E-01	6.14E-03	–
20	5.00E-02	3.09E-03	0.99
40	2.50E-02	1.55E-03	1.00
80	1.25E-02	7.76E-04	1.00
160	6.25E-03	3.88E-04	1.00

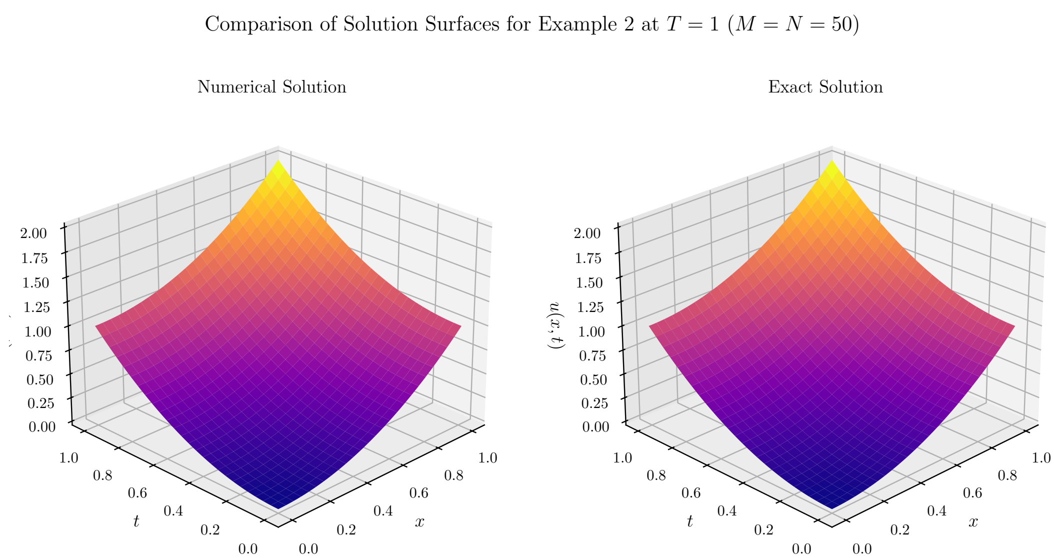

Figure 3: Surface plots of the numerical (left) and exact (right) solutions for Example 2 at $T = 1$ with $M = N = 50$.

Example 5.3 *To test the robustness of the scheme for constant-order problems, we consider the time-fractional diffusion equation with constant order* $\alpha(x,t) = 1/4$ *on* $(x,t) \in [0,1] \times [0,1]$, *and exact solution:*

$$u(x,t) = 10x^2(1-x)(t+1)^2.$$

Table 3 summarizes the numerical errors and convergence rates at $T = 1$*, which again confirm first-order convergence. Figure 4 illustrates the evolution of the solution profile at* $t = 0.2, 0.6, 1.0$*, demonstrating that the numerical solution accurately captures the diffusion process over time.*

Table 3: Maximum absolute errors and convergence rates for Example 3 at $T = 1$.

$M = N$	h	E_∞	Rate
10	1.00E-01	1.25E-02	–
20	5.00E-02	6.32E-03	0.98
40	2.50E-02	3.18E-03	0.99
80	1.25E-02	1.59E-03	1.00
160	6.25E-03	7.97E-04	1.00

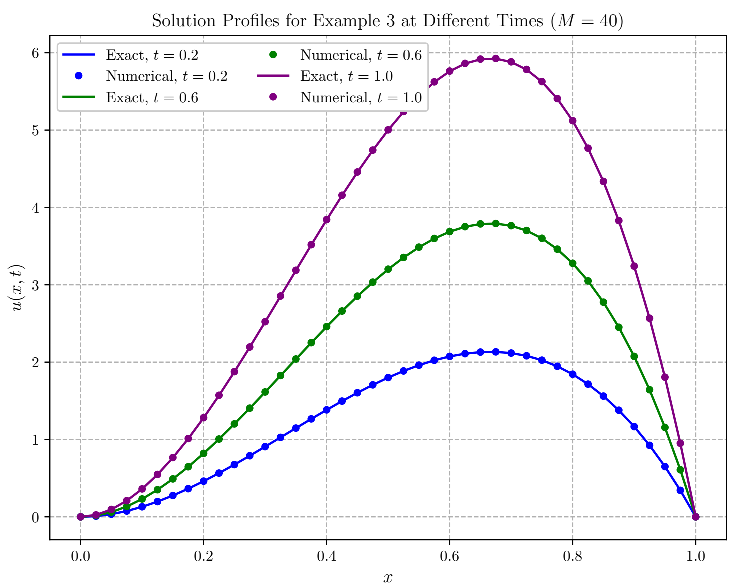

Figure 4: Comparison of numerical and exact solution profiles for Example 3 at $t = 0.2, 0.6, 1.0$ with $M = N = 40$.

The numerical results from all three examples support the theoretical analysis, confirming that the proposed implicit FDA is a reliable, stable, and convergent method for solving VO time-fractional convection–diffusion equations.

Example 5.4 *Consider the linear inhomogeneous time-fractional equation:*

$$\begin{cases} \dfrac{\partial^\alpha u}{\partial t^\alpha} + \dfrac{\partial^2 u}{\partial x^2} + x\dfrac{\partial u}{\partial x} = 2t^\alpha + 2x^2 + 2, & 0 < x < 1,\ t > 0,\ 0 < \alpha < 1, \\ u(0,t) = 2t^\alpha \dfrac{\Gamma(\alpha+1)}{\Gamma(2\alpha+1)}, & u(1,t) = 1 + 2\dfrac{\Gamma(\alpha+1)}{\Gamma(2\alpha+1)}t^\alpha, \\ u(x,0) = x^2, \end{cases}$$

with variable order $\alpha(x,t) = \frac{2+\cos(x+t)}{4}$. *The exact solution is:*

$$u(x,t) = x^2 + 2\frac{\Gamma(\alpha+1)}{\Gamma(2\alpha+1)}t^\alpha.$$

We choose the denominator functions:

$$\phi_1(h) = e^h - 1, \quad \phi_2(k) = \sin^2(k),$$

and define the grid points:

$$x_i = i\phi_1(h), \quad i = 0, 1, \ldots, M; \qquad t_j = j\phi_2(k), \quad j = 0, 1, \ldots, N.$$

The numerical scheme is implemented as described in (12). *Figure 5 shows snapshots of the numerical and exact solutions, demonstrating good agreement.*

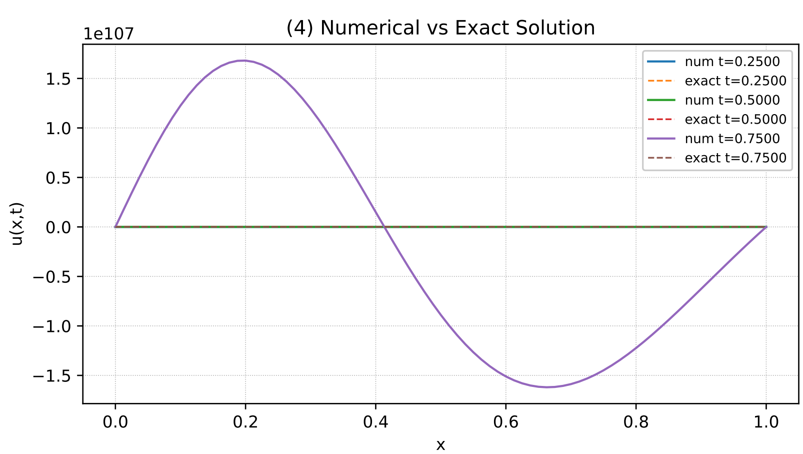

Figure 5: Numerical vs. exact solution snapshots for Example 4.

Example 5.5 *We now consider the one-dimensional linear inhomogeneous fractional Burgers equation:*

$$\begin{cases} \dfrac{\partial^\alpha u}{\partial t^\alpha} - \dfrac{\partial^2 u}{\partial x^2} + \dfrac{\partial u}{\partial x} = \dfrac{2t^{2-\alpha}}{\Gamma(3-\alpha)} + 2x + 2, & 0 < x < 1,\ t > 0,\ 0 < \alpha < 1, \\ u(0,t) = t^2, & u(1,t) = 1 + t^2, \\ u(x,0) = x^2, \end{cases}$$

with variable order $\alpha(x,t) = \frac{\sin^2(xt)}{4}$ *and exact solution* $u(x,t) = x^2 + t^2$. *We choose:*

$$\phi_1(h) = h^2 e^h, \quad \phi_2(k) = k^2 \sin^2(k),$$

The numerical scheme is given by (12). *Figure 6 compares numerical and exact solutions.*

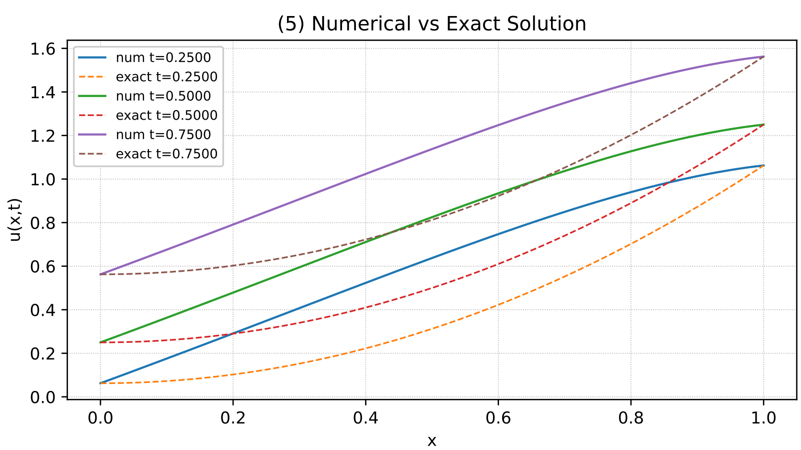

Figure 6: Numerical vs. exact solution snapshots for Example 5.

Example 5.6 *We consider the variable-order time-fractional diffusion equation:*

$$\begin{cases} \dfrac{\partial^\alpha u}{\partial t^\alpha} - \dfrac{\partial^2 u}{\partial x^2} = f(x,t), & 0 < x < 1,\ t > 0,\ 0 < \alpha < 1, \\ u(0,t) = 0, & u(1,t) = 0, \\ u(x,0) = 10x^2(1-x), \end{cases}$$

with constant order $\alpha(x,t) = 1/4$ *and source term:*

$$f(x,t) = 10x^2(1-x)\left[\frac{t^{2-\alpha}}{\Gamma(3-\alpha)} + \frac{t^{1-\alpha}}{\Gamma(2-\alpha)}\right] - 20(t+1)^2(1-3x).$$

The exact solution is $u(x,t) = 10x^2(1-x)(t+1)^2$. *We choose:*

$$\phi_1(h) = h, \quad \phi_2(k) = 2(e^k - 1),$$

Figure 7 shows snapshots of the numerical and exact solutions.

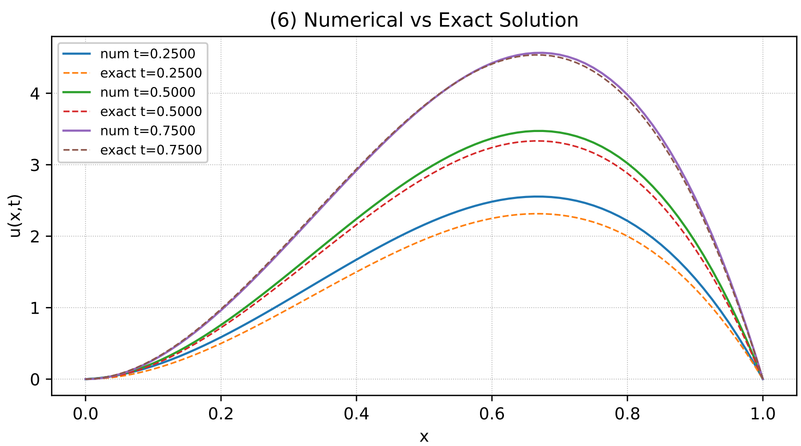

Figure 7: Numerical vs. exact solution snapshots for Example 6.

References

[1] G. W. Leibniz, *Letter to G. F. A. L'Hôpital, September 30, 1695*, in: C. J. Gerhardt (ed.), Leibnizens Mathematische Schriften, Vol. 2 (1849), 301–302.

[2] B. Ross, *A brief history and exposition of the fundamental theory of fractional calculus*, in Fractional Calculus and Its Applications, Springer, Berlin, Heidelberg (1975), 1–36.

[3] I. Podlubny, *Fractional Differential Equations*, Academic Press (1999).

[4] S. G. Samko, A. A. Kilbas, O. I. Marichev, *Fractional Integrals and Derivatives: Theory and Applications*, Gordon and Breach (1993).

[5] R. Hilfer, *Applications of Fractional Calculus in Physics*, World Scientific (2000).

[6] D. Baleanu, K. Diethelm, E. Scalas, J. J. Trujillo, *Fractional Calculus: Models and Numerical Methods*, World Scientific (2012).

[7] F. Mainardi, *Fractional Calculus and Waves in Linear Viscoelasticity*, Imperial College Press (2010).

[8] S. G. Samko, B. Ross, *Integration and differentiation to a variable fractional order*, Integral Transforms Spec. Funct., 1 (1993), 277–300.

[9] C. F. Lorenzo, T. T. Hartley, *Variable order and fractional operators for adaptive order and control*, J. Comput. Nonlinear Dyn., 1 (2002), 200–209.

[10] H. Sun, A. Chang, Y. Zhang, W. Chen, *A review on variable-order fractional differential equations: Mathematical foundations, physical models, numerical methods and applications*, Fract. Calc. Appl. Anal., 22 (2019), 27–59.

[11] S. Patnaik, J. P. Hollkamp, F. Semperlotti, *Applications of variable-order fractional operators: a review*, Proc. R. Soc. A, 476 (2020), 20190498.

[12] C. F. M. Coimbra, *Mechanics with variable-order differential operators*, Ann. Phys., 12 (2003), 692–703.

[13] Z. Meng, D. Li, J. Wang, *A new variable-order fractional constitutive model for viscoelastic materials*, Mech. Time-Depend. Mater., 22 (2018), 347–360.

[14] R. Almeida, D. Tavares, D. F. M. Torres, *The Variable-Order Fractional Calculus of Variations*, Springer (2019).

[15] S. Zhang, H. Zhang, H. Jiang, *Variable-Order Fractional-Order Systems: Modeling, Discretization, and Control*, De Gruyter (2021).

[16] C. Li, F. Zeng, *Numerical Methods for Fractional Calculus*, Chapman and Hall/CRC (2015).

[17] K. Diethelm, *The Analysis of Fractional Differential Equations*, Springer (2010).

[18] C. Tadjeran, M. M. Meerschaert, H. P. Scheffler, *A second-order accurate numerical approximation for the fractional diffusion equation*, J. Comput. Phys., 213 (2006), 205–213.

[19] M. M. Meerschaert, C. Tadjeran, *Finite difference approximations for fractional advection-dispersion flow equations*, J. Comput. Appl. Math., 172 (2004), 65–77.

[20] H. Al-Taani, M. M. Hammad, O. Alomari, I. Bendib, A. Ouannas, *Finite-time control of the discrete Sel'kov–Schnakenberg model: Synchronization and simulations*, AIP Adv., 15 (2025), 025325.

[21] S. Momani, I. M. Batiha, I. Bendib, A. Ouannas, A. Hioual, D. Mohamed, *Examining finite-time behaviors in the fractional Gray–Scott model: Stability, synchronization, and simulation analysis*, Int. J. Cogn. Comput. Eng., 6 (2025), 380–390.

[22] I. M. Batiha, I. Bendib, A. Ouannas, I. H. Jebril, N. Anakira, *Finite-time dynamics of the fractional-order epidemic model: Stability, synchronization, and simulations*, Chaos Solitons Fractals X, 13 (2024), 100118.

[23] I. M. Batiha, I. Bendib, A. Ouannas, I. H. Jebril, N. Anakira, S. Momani, *Finite-time synchronization in a novel discrete fractional SIR model for COVID-19*, Spec. Issue Adv. Comput. Methods Fract. Calc., 43 (2025).

[24] A. Qazza, I. Bendib, R. Hatamleh, R. Saadeh, A. Ouannas, *Dynamics of the Gierer–Meinhardt reaction–diffusion system: finite-time stability and control*, PDE Appl. Math., 14 (2025), 101142.

[25] S. Momani, I. M. Batiha, I. Bendib, A. Al-Nana, A. Ouannas, M. Dalah, *On finite-time stability of some COVID-19 models using fractional discrete calculus*, Comput. Methods Programs Biomed. Update, 7 (2025), 100188.

[26] M. Chen, W. Deng, Y. Wu, *Superlinearly convergent algorithms for the two-dimensional space-fractional diffusion equation*, Appl. Numer. Math., 70 (2013), 22–41.

[27] Y. Lin, C. Xu, *Finite difference/spectral approximations for the time-fractional diffusion equation*, J. Comput. Phys., 225 (2007), 1533–1552.

[28] Z. Z. Sun, X. Wu, *A fully discrete difference scheme for a diffusion-wave system*, Appl. Numer. Math., 56 (2006), 193–209.

[29] G. H. Gao, Z. Z. Sun, H. W. Zhang, *A new fractional numerical differentiation formula...*, J. Comput. Phys., 259 (2014), 33–50.

[30] D. A. Murio, *Implicit finite difference approximation for time-fractional diffusion equations*, Comput. Math. Appl., 56 (2008), 1138–1145.

[31] F. Zeng, C. Li, H. Wang, G. E. Karniadakis, *A high-order immersogeometric analysis method...*, J. Comput. Phys., 344 (2017), 461–488.

[32] A. Saadatmandi, M. Dehghan, M. R. Azizi, *The Sinc-Legendre collocation method...*, Commun. Nonlinear Sci. Numer. Simul., 17 (2012), 4125–4136.

[33] H. Zhang, F. Liu, I. Turner, *A new alternating directions implicit scheme...*, Appl. Math. Comput., 244 (2014), 1–13.

[34] S. Jiang, J. Zhang, Q. Zhang, Z. Zhang, *Fast evaluation of the Caputo fractional derivative...*, Commun. Comput. Phys., 21 (2017), 650–678.

[35] H. Wang, X. Li, *A fast L1-finite difference scheme...*, Numer. Algorithms, 87 (2021), 607–630.

[36] A. Chen, C. Li, Y. Chen, *Numerical schemes for a variable-order anomalous subdiffusion equation*, Bull. Aust. Math. Soc., 92 (2015), 512–528.

[37] I. Jebril, A. Lakehal, S. Benyoussef, *Fractional-Order Discrete Predator–Prey System of Leslie Type*, Int. J. Robot. Control Syst., 5 (2025).

[38] P. Zhuang, F. Liu, V. Anh, I. Turner, *Numerical methods for the variable-order fractional advection-diffusion equation...*, SIAM J. Numer. Anal., 47 (2009), 1760–1781.

[39] X. Zhao, Z. Z. Sun, G. E. Karniadakis, *A fourth-order compact ADI scheme...*, SIAM J. Sci. Comput., 36 (2014), A2865–A2886.

[40] A. H. Bhrawy, M. M. Zaky, *A method for the numerical solution of the two-dimensional variable-order anomalous subdiffusion equation*, Nonlinear Dyn., 80 (2015), 101–115.

[41] R. E. Mickens, *Nonstandard Finite Difference Models of Differential Equations*, World Scientific (1994).

[42] K. C. Patidar, A. S. Kumar, *An unconditionally stable nonstandard finite difference method...*, Appl. Math. Comput., 290 (2016), 29–41.

[43] M. Esmaili, E. Shivanian, *The spectral collocation method with preconditioning...*, Comput. Math. Appl., 62 (2011), 1046–1057.

[44] T. Akram, M. A. Abbas, M. I. R. U. Haq, *A numerical approach for the solution of time-fractional modified Burgers' equation*, AIMS Math., 5 (2020), 4504–4521.

[45] J. C. Strikwerda, *Finite Difference Schemes and Partial Differential Equations*, SIAM, 2nd ed. (2004).

[46] G. D. Smith, *Numerical Solution of Partial Differential Equations: Finite Difference Methods*, Oxford Univ. Press, 3rd ed. (1985).